Volume 7 | Number 6 | 14 February 2016 | Pages 1209–1346

Polymer Chemistry

www.rsc.org/polymers

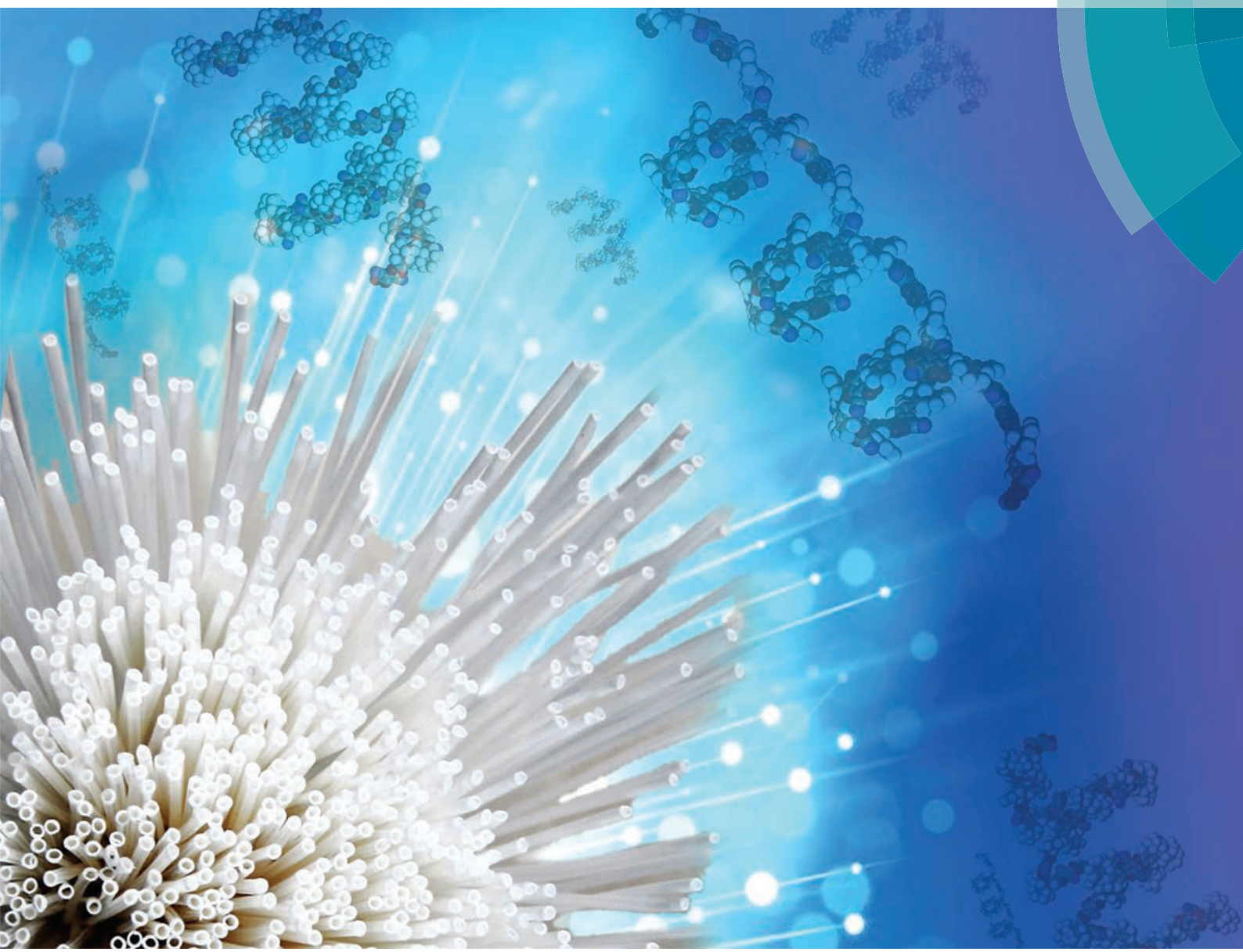

ISSN 1759-9954

ROYAL SOCIETY OF CHEMISTRY

PAPER
Xiaohua Ma and Ingo Pinnau
A novel intrinsically microporous ladder polymer and copolymers derived from 1,1′,2,2′-tetrahydroxy-tetraphenylethylene for membrane-based gas separation

175 YEARS

Polymer Chemistry

PAPER

View Article Online
View Journal | View Issue

CrossMark click for updates

Cite this: *Polym. Chem.*, 2016, **7**, 1244

A novel intrinsically microporous ladder polymer and copolymers derived from 1,1′,2,2′-tetrahydroxy-tetraphenylethylene for membrane-based gas separation†

Xiaohua Ma and Ingo Pinnau*

Received 9th November 2015,
Accepted 8th December 2015

DOI: 10.1039/c5py01796c

www.rsc.org/polymers

A novel intrinsically microporous polymer was synthesized by polycondensation reaction of 1,1′,2,2′,-tetrahydroxy-tetraphenylethylene (TPE) and 2,3,5,6-tetrafluoroterephthalonitrile (TFTPN). In addition, a series of copolymers was prepared from TPE, 5,5′,6,6′-tetrahydroxy-3,3,3′,3′-tetramethylspirobisindane (TTSBI) and TFTPN. All TPE-derived polymers exhibited high molecular weight, good solubility in common organic solvents, high thermal stability and high surface area (550 to 660 $m^2\ g^{-1}$). The CO_2 permeability of a methanol-treated and 120 °C vacuum-dried TPE-TFTPN film was 862 Barrer with a moderate CO_2/N_2 selectivity of 26. The selectivity of the TPE-TTSBI-PIMs decreased with increasing TTSBI content coupled with a sharp increase in permeability. Molecular simulations indicated that the introduction of the tetraphenylethylene unit resulted in an increased rotational freedom of dihedral angles in the polymer main chain relative to those of the spirobisindane-based PIM-1.

Published on 09 Muddee 2015. Downloaded on 07/08/2025 8:31:58 PM.

Introduction

In recent years, there has been increasing interest in the synthesis of porous polymers, such as conjugated porous polymers, covalent organic frameworks, crosslinked porous polymers and intrinsically microporous polymers.[1–3] Their microporosity and design flexibility can potentially be exploited in a variety of fields such as catalysis,[2,3] sensors for trace substance detection,[4] energy conversion and storage,[5,6] and membrane-based separation.[7,8] Among the above materials, polymers of intrinsic microporosity (PIM) are the most promising porous polymer class for membrane applications, due to their combination of high permeability and selectivity as well as good solution processability.[8–10]

Glassy ladder polymers of intrinsic microporosity were first introduced in 2004 by McKeown's and Budd's group.[9,10] The state-of-the-art PIM-1 was formed by simple condensation polymerization of 5,5′,6,6′-tetrahydroxy-3,3,3′,3′-tetramethylspirobisindane (TTSBI) and 2,3,5,6-tetrafluoroterephthalonitrile (TFTPN). The resulting polymer was composed of rigid ladder-type repeat units including bulky, sterically hindered spirobisindane contortion sites. As a result, PIM-1 showed highly inefficient chain packing with a remarkable microporosity, as determined by nitrogen adsorption measurements at −196 °C ($S_{BET} \sim 800\ m^2\ g^{-1}$).

PIM-1 exhibited over 100-fold enhanced permeability compared to commercial low-free-volume polymers, such as Matrimid,[11] coupled with a modest selectivity. The gas permeation properties of PIM-1 reached the 2008 Robeson permeability/selectivity upper bound for some gas pairs.[12–15] Based on the promising results obtained for PIM-1, many other high-performance ladder PIMs,[16–29] modified prototype PIM-1,[30–33] and PIM polyimides (PIM-PI)[34–42] have been reported with excellent gas separation properties. In fact, several ladder PIMs[25–27] and PIM-PIs[37,40,41] demonstrated much better performance than other known polymers, thereby redefining the previously reported permeability/selectivity upper bound for air and hydrogen separation.[27] However, in the burgeoning materials class of PIMs there is still a quest for novel custom-designed building blocks to further improve the understanding of structure/property relationships for advanced gas separation membranes.

Tetraphenylethylene (TPE) is a building block widely investigated in aggregation-induced emission (AIE) materials, which originated from the restriction of the intramolecular rotation (RIR) effect in the tetraphenylethylene moiety.[43,44] TPE is a bulky and sterically hindered group with great potential as a building block for the development of novel PIMs for

Advanced Membranes and Porous Materials Center, Physical Sciences and Engineering Division, Chemical and Biological Engineering Program, King Abdullah University of Science and Technology, Thuwal 23955-6900, Saudi Arabia.
E-mail: ingo.pinnau@kaust.edu.sa; Fax: +966 012 80821328

†Electronic supplementary information (ESI) available: The synthesis details, solubility, membrane formation, testing protocol and upper bound plots of the homo- and co-PIMs for different gas pairs. See DOI: 10.1039/c5py01796c

This journal is © The Royal Society of Chemistry 2016

Published on 09 Muddee 2015. Downloaded on 07/08/2025 8:31:58 PM.

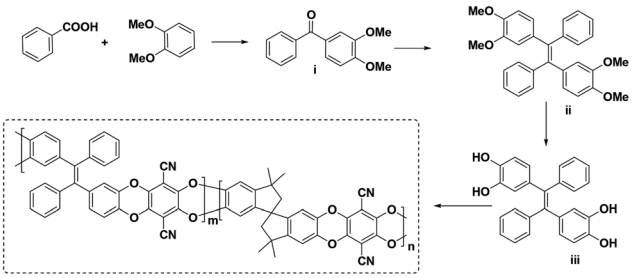

Scheme 1 Design and synthesis of tetraphenylethylene-based homo-PIM and co-PIMs. m = 1, n = 0 (TPE-TFTPN); m = 0, n = 1 (TTSBI-TFTPN = PIM-1).

membrane-based separation. In this study, we report for the first time the design and synthesis of tetraphenylethylene-based PIMs, as illustrated in Scheme 1. The detailed synthetic procedure and characterization are provided in the ESI.†

Results and discussion

(3,4-Dimethoxyphenyl) (phenyl)methanone **i** was synthesized by a previously reported method[22] and was then converted to 1,1′,2,2′-tetramethoxy-tetraphenylethylene *via* the McMurry reaction in the presence of zinc and $TiCl_4$ as catalysts.[45] The McMurray reaction for the asymmetric ketone ((3,4-dimethoxyphenyl)(phenyl)methanone) resulted in *trans* and *cis* isomers with a ratio of 85/15. The *trans* isomer was separated by column chromatography and the pure product was used for further reactions (Scheme S1 and Fig. S1†). The resulting intermediate **ii** was further demethylated with BBr_3, and monomer **iii** was obtained quantitatively. This monomer and 5,5′,6,6′-tetrahydroxy-3,3,3′,3′-tetramethylspirobisindane (TTSBI) were polymerized in different ratios with 2,3,5,6-tetrafluoroterephthalonitrile (TFTPN) in DMAc as a solvent and K_2CO_3 as a base at 140 °C for 5 to 10 min. A series of homo- and co-PIMs denoted as TPE-PIM, TPE-75, TPE-50, TPE-25 and PIM-1 were obtained with the corresponding TPE ratios of 100, 75, 50, 25 and 0 percent. The ratios of the homo- and co-PIMs were characterized and identified by NMR, as shown in Fig. 1.

The resulting co-PIMs demonstrated good solubility in some common solvents such as THF, dichloromethane, chloroform, NMP, DMF, and DMAc (Table S1†). These polymers exhibited high molecular weight (M_n), ranging from 3.4 × 10^4 to 14.5 × 10^4 g mol^{-1}, coupled with a polydispersity of 2.1 to 3.2, as determined by GPC using chloroform as the solvent. Transparent, yellow films were made by casting a 2–3% (wt/v) chloroform solution into leveled Petri dishes and evaporating the solvent under ambient conditions. The films were then soaked in methanol for 24 hours to remove any trapped casting solvent. Thereafter, the films were dried at 120 °C under vacuum for 24 h. TGA experiments confirmed that the films were solvent-free prior to the gas permeation tests.

Similar to previously reported microporous PIMs,[18] all of the homo- and co-PIMs of this study exhibited completely amorphous structures as identified by wide-angle X-ray scattering shown in Fig. 2. TPE-PIM demonstrated tighter chain packing compared with PIM-1, as indicated by the much weaker peak at a low-angle around 13.6° (d-spacing = 6.5 Å), whereas higher intensity is evident at an angle of around 20° (d-spacing = 4.4 Å). As expected, the copolymers show X-ray scattering between those of the homopolymers, depending on the TPE/TTSBI ratio (Fig. 2).

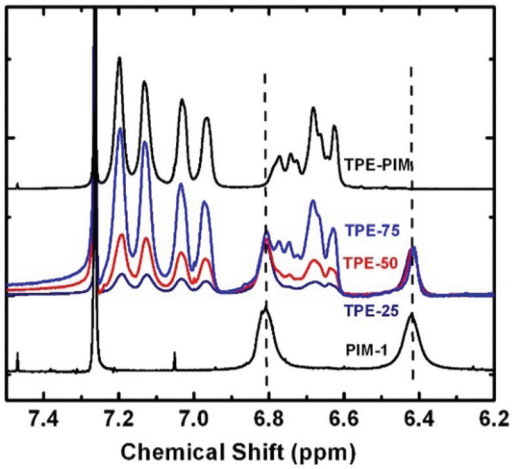

Fig. 1 Proton NMR of TPE-PIM, PIM-1 and TPE-PIM-1 copolymers; the peaks of the copolymers were normalized at 6.41 ppm.

All TPE-based PIMs demonstrated high thermal stability as identified from their onset decomposition temperature over 440 °C, as illustrated in Fig. 3. It is interesting to note that TPE-PIM had a 40 °C higher decomposition temperature than PIM-1, most likely due to its higher aromatic content.

The TPE-based PIMs demonstrated high surface area (Table 1), which was calculated from their N_2 adsorption iso-

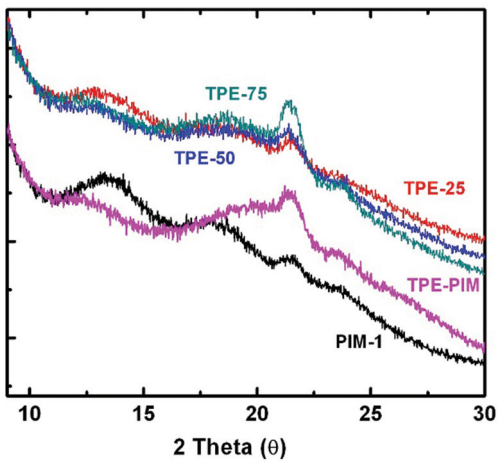

Fig. 2 Wide-angle X-ray scattering of TPE-PIM, PIM-1 and copolymers. TPE-25, TPE-50 and TPE-75 were normalized and shifted in the y-axial direction above PIM-1 and TPE-PIM.

Published on 09 Muddee 2015. Downloaded on 07/08/2025 8:31:58 PM.

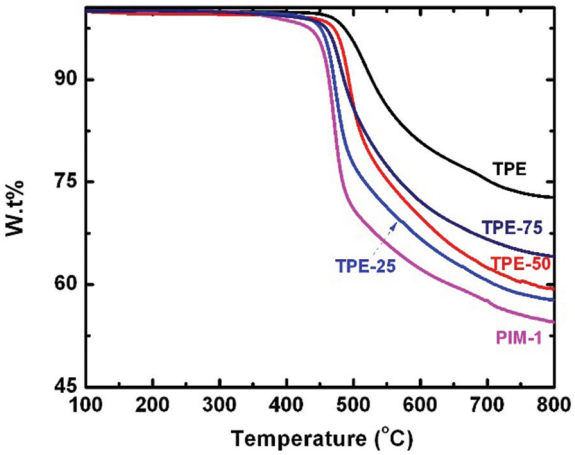

Fig. 3 Thermal gravimetric analysis of the TPE-based PIMs and PIM-1.

Table 1 Basic properties of TPE-PIM, PIM-1 and TPE-PIM copolymers

Polymers	$M_n \times 10^{-4}$ [a] (g mol^{-1})	PDI[b]	T_d [c] (°C)	S_{BET} (m^2 g^{-1})	Total pore volume[d]
TPE-PIM	7.83	2.3	475	550	0.54
TPE-75	3.40	3.2	465	560	0.47
TPE-50	6.00	2.1	455	600	0.45
TPE-25	4.90	2.3	440	660	0.51
PIM-1	14.5	2.4	430	770	0.70

[a] The molecular weight of the polymers was measured by GPC using chloroform as the solvent and polystyrene as the external standard. The eluent speed was 1 mL min^{-1}. [b] The PDI was obtained by M_w/M_n. [c] The decomposition temperature was selected as the onset decomposition temperature of the TGA curve. [d] The total pore volume was obtained at the relative N_2 pressure (p/p_0) of 0.97.

therms at −196 °C, as illustrated in Fig. 4. All polymers exhibited type I adsorption isotherms characterized by remarkable sorption uptake at very low relative pressure ($p/p_0 < 0.01$), indicating the presence of significant microporosity. TPE-PIM had the lowest surface area of 550 m^2 g^{-1} of all polymers reported in this study. As the fraction of the spirobisindane repeat unit increased in the copolymers, a significant increase in the adsorption uptake at a relatively low pressure ($p/p_0 < 0.1$) was observed, and the surface area of the TPE-based PIMs increased continuously from 550 m^2 g^{-1} (TPE-PIM) to 770 m^2 g^{-1} (PIM-1).

In order to evaluate the performance of TPE-based PIMs, the gas transport properties of the polymers were analyzed by the constant-volume/variable-pressure method. The data are summarized in Table 2. The permeability and selectivity values of PIM-1 were similar to those reported by Du *et al.* for the films prepared under similar conditions.[18] A sharp decrease in permeability was observed for all gases when the tetraphenylethylene moiety was substituted for spirobisindane in the PIM copolymers. For example, TPE-PIM had a CO_2 permeability of 862 Barrer, which is about 7-fold lower than PIM-1. However, there is a concurrent improvement in selectivity, *e.g.* the selectivity of O_2/N_2 and CO_2/CH_4 improved from 3.2 to 4.2 and 12 to 21, respectively. The sequence of the gas permeability of all polymers in this study was $P_{CO_2} > P_{H_2} > P_{O_2} > P_{CH_4} > P_{N_2}$, which is typically observed for high surface area PIMs. It is interesting to note that there is a qualitative correlation between the permeability and the surface area of the polymers, that is higher BET surface area was coupled with higher gas permeability and lower gas selectivity by increasing the spirobisindane content in the TPE-copolymers (Table 2).

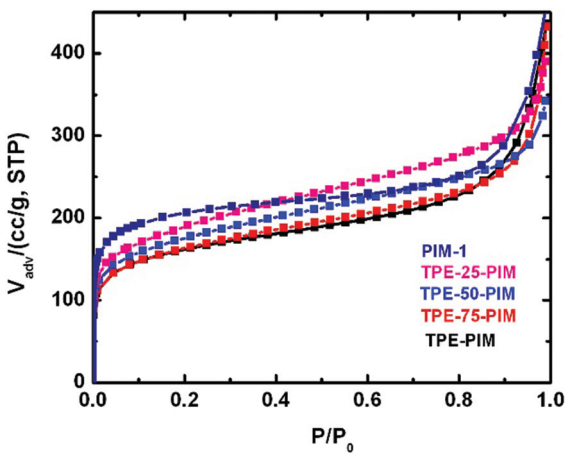

Fig. 4 N_2 adsorption isotherms of the TPE-Based PIMs and PIM-1 at −196 °C.

Table 2 Gas permeability and ideal selectivity of TPE-PIM, TPE-PIM-1 copolymers and PIM-1 (2 bar; 35 °C)

		Permeability (Barrer)[b]				Ideal selectivity ($\alpha_{X/Y}$)			
Polymer[a]	H_2	N_2	O_2	CH_4	CO_2	H_2/N_2	O_2/N_2	CO_2/N_2	CO_2/CH_4
TPE-PIM	604	33.4	138	41	862	18	4.2	25.8	20.9
TPE-75	620	42	154	61	977	15	3.7	23.3	16
TPE-50	1004	88	288	134	1869	11	3.4	21.3	14
TPE-25	2332	256	836	415	5203	9	3.3	20.3	12.5
PIM-1	3017	350	1103	495	5922	8.6	3.2	16.9	12.0

[a] The membranes were cast using chloroform as the solvent and soaked in methanol for 24 hours, and thereafter dried under vacuum at 120 °C for 24 h. [b] 1 Barrer = 10^{-10} cm^3 (STP) cm cm^{-2} s^{-1} cm Hg^{-1} = 7.5×10^{-18} m^3 (STP) m m^{-2} s^{-1} Pa^{-1}.

 This journal is © The Royal Society of Chemistry 2016

Published on 09 Muddee 2015. Downloaded on 07/08/2025 8:31:58 PM.

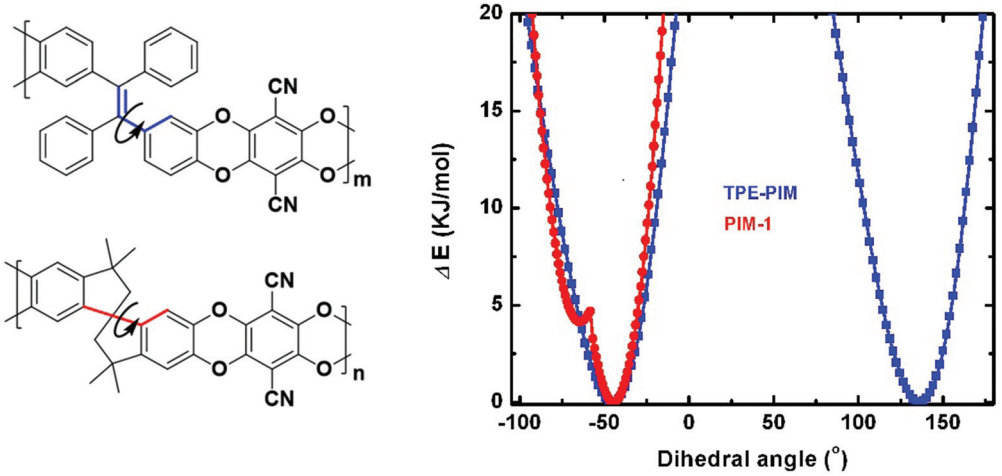

Fig. 5 The rotation angles selected in TPE-PIM (blue) and PIM-1 (red) and their calculated rotation energy against dihedral angle.

The permeability/selectivity trade-off plots for O_2/N_2, CO_2/CH_4, CO_2/N_2 and H_2/N_2 are illustrated in Fig. S2.† The TPE-based PIMs and co-PIMs are located below the 2008 and 2015 permeability/selectivity trade-off curves. It is suggested that the rotational freedom of the ethylene bond in the TPE-PIM repeat unit leads to more efficient polymer packing and, hence lower free volume and permeability. The calculated rotation energies of the dihedral angle of the tetraphenylethylene and spirobisindane units are highlighted in Fig. 5. When the dihedral angle was rotated from −180 to +180°, two energy minima for TPE-PIM, both at the positive dihedral angle of 130° and a negative dihedral angle around −50°, were observed. In the case of PIM-1, owing to its fused ring structure, only one energy minimum at around −50° was observed. Therefore, the conformational freedom of TPE-PIM is much larger than that of PIM-1, resulting in a more densely packed polymer structure.

Conclusions

A novel TPE-based monomer was synthesized by the McMurry method and successfully introduced as a building block for the synthesis of polymers of intrinsic microporosity. A TPE-based homopolymer and a series of co-PIMs were prepared by reaction of TPE with 5,5′,6,6′-tetrahydroxy-3,3,3′,3′-tetramethylspirobisindane (TTSBI) and 2,3,5,6-tetrafluoroterephthalonitrile (TFTPN). The amorphous glassy TPE-based PIMs demonstrated good solubility and higher thermal stability than PIM-1. Their BET surface area was in the range of 550 to 660 $m^2\ g^{-1}$. The TPE-based PIMs showed lower permeability coupled with a moderately enhanced selectivity compared with PIM-1. The WAXD results showed a tighter structure of TPE-PIM and its copolymers as indicated by smaller *d*-spacing values than observed in PIM-1. Molecular simulations demonstrated that TPE-PIMs have more rotational freedom than PIM-1, which is likely to be the cause for a denser structure, and hence lower permeability.

Acknowledgements

This research was supported by KAUST baseline funding for Prof. Ingo Pinnau (BAS/1/1323-01-01).

Notes and references

1 Y. Xu, S. Jin, H. Xu, A. Nagai and D. Jiang, *Chem. Soc. Rev.*, 2013, **42**, 8012–8031.
2 D. Wu, F. Xu, B. Sun, R. Fu, H. He and K. Matyjaszewski, *Chem. Rev.*, 2012, **112**, 3959–4015.
3 S. Lin, C. S. Diercks, Y. B. Zhang, N. Kornienko, E. M. Nichols, Y. Zhao, A. R. Paris, D. Kim, P. Yang, O. M. Yaghi and C. J. Chang, *Science*, 2015, **349**, 1208–1213.
4 Y. Wang, N. B. McKeown, K. J. Msayib, G. A. Turnbull and I. D. Samuel, *Sensors*, 2011, **11**, 2478–2487.
5 F. Vilela, K. Zhang and M. Antonietti, *Energy Environ. Sci.*, 2012, **5**, 7819.
6 N. Du, H. B. Park, M. M. Dal-Cin and M. D. Guiver, *Energy Environ. Sci.*, 2012, **5**, 7306–7322.
7 N. B. McKeown and P. M. Budd, *Chem. Soc. Rev.*, 2006, **35**, 675–683.
8 R. W. Baker and B. T. Low, *Macromolecules*, 2014, **47**, 6999–7013.
9 P. M. Budd, E. S. Elabas, B. S. Ghanem, S. Makhseed, N. B. McKeown, K. J. Msayib, C. E. Tattershall and D. Wang, *Adv. Mater.*, 2004, **16**, 456–459.
10 P. M. Budd, B. S. Ghanem, S. Makhseed, N. B. McKeown, K. J. Msayib and C. E. Tattershall, *Chem. Commun.*, 2004, 230–231.
11 W. J. Koros and G. K. Fleming, *J. Membr. Sci.*, 1993, **83**, 1–80.
12 P. Budd, K. Msayib, C. Tattershall, B. Ghanem, K. Reynolds, N. McKeown and D. Fritsch, *J. Membr. Sci.*, 2005, **251**, 263–269.

Published on 09 Muddee 2015. Downloaded on 07/08/2025 8:31:58 PM.

13 P. Budd, N. McKeown, B. Ghanem, K. Msayib, D. Fritsch, L. Starannikova, N. Belov, O. Sanfirova, Y. Yampolskii and V. Shantarovich, *J. Membr. Sci.*, 2008, **325**, 851–860.
14 L. M. Robeson, *J. Membr. Sci.*, 2008, **320**, 390–400.
15 L. M. Robeson, Z. P. Smith, B. D. Freeman and D. R. Paul, *J. Membr. Sci.*, 2014, **453**, 71–83.
16 N. Du, G. P. Robertson, J. Song, I. Pinnau, S. Thomas and M. D. Guiver, *Macromolecules*, 2008, **41**, 9656–9662.
17 N. Du, G. P. Robertson, I. Pinnau and M. D. Guiver, *Macromolecules*, 2009, **42**, 6023–6030.
18 N. Du, G. P. Robertson, I. Pinnau and M. D. Guiver, *Macromolecules*, 2010, **43**, 8580–8587.
19 M. Carta, K. J. Msayib, P. M. Budd and N. B. McKeown, *Org. Lett.*, 2008, **10**, 2641–2643.
20 R. Short, M. Carta, C. G. Bezzu, D. Fritsch, B. M. Kariuki and N. B. McKeown, *Chem. Commun.*, 2011, **47**, 6822–6824.
21 M. Carta, P. Bernardo, G. Clarizia, J. C. Jansen and N. B. McKeown, *Macromolecules*, 2014, **47**, 8320–8327.
22 C. G. Bezzu, M. Carta, A. Tonkins, J. C. Jansen, P. Bernardo, F. Bazzarelli and N. B. McKeown, *Adv. Mater.*, 2012, **24**, 5930–5933.
23 I. Rose, M. Carta, R. Malpass-Evans, M.-C. Ferrari, P. Bernardo, G. Clarizia, J. C. Jansen and N. B. McKeown, *ACS Macro Lett.*, 2015, **4**, 912–915.
24 B. S. Ghanem, N. B. McKeown, P. M. Budd and D. Fritsch, *Macromolecules*, 2008, **41**, 1640–1646.
25 M. Carta, R. Malpass-Evans, M. Croad, Y. Rogan, J. C. Jansen, P. Bernardo, F. Bazzarelli and N. B. McKeown, *Science*, 2013, **339**, 303–307.
26 M. Carta, M. Croad, R. Malpass-Evans, J. C. Jansen, P. Bernardo, G. Clarizia, K. Friess, M. Lanc and N. B. McKeown, *Adv. Mater.*, 2014, **26**, 3526–3531.
27 B. S. Ghanem, R. Swaidan, X. H. Ma, E. Litwiller and I. Pinnau, *Adv. Mater.*, 2014, **26**, 6696–6700.
28 S. Liu, Z. Jin, Y. C. Teo and Y. Xia, *J. Am. Chem. Soc.*, 2014, **136**, 17434–17437.
29 Z. G. Wang, X. Liu, D. Wang and J. Jin, *Polym. Chem.*, 2014, **5**, 2793.
30 N. Du, G. P. Robertson, J. Song, I. Pinnau and M. D. Guiver, *Macromolecules*, 2009, **42**, 6038–6043.
31 N. Du, H. B. Park, G. P. Robertson, M. M. Dal-Cin, T. Visser, L. Scoles and M. D. Guiver, *Nat. Mater.*, 2011, **10**, 372–375.
32 C. R. Mason, L. Maynard-Atem, N. M. Al-Harbi, P. M. Budd, P. Bernardo, F. Bazzarelli, G. Clarizia and J. C. Jansen, *Macromolecules*, 2011, **44**, 6471–6479.
33 C. R. Mason, L. Maynard-Atem, K. W. J. Heard, B. Satilmis, P. M. Budd, K. Friess, M. Lanč, P. Bernardo, G. Clarizia and J. C. Jansen, *Macromolecules*, 2014, **47**, 1021–1029.
34 B. S. Ghanem, N. B. McKeown, P. M. Budd, J. D. Selbie and D. Fritsch, *Adv. Mater.*, 2008, **20**, 2766–2771.
35 Y. Rogan, R. Malpass-Evans, M. Carta, M. Lee, J. C. Jansen, P. Bernardo, G. Clarizia, E. Tocci, K. Friess, M. Lanč and N. B. McKeown, *J. Mater. Chem. A*, 2014, **2**, 4874.
36 Z. Wang, D. Wang, F. Zhang and J. Jin, *ACS Macro Lett.*, 2014, **3**, 597–601.
37 X. Ma, B. Ghanem, O. Salines, E. Litwiller and I. Pinnau, *ACS Macro Lett.*, 2015, **4**, 231–235.
38 X. Ma, B. Ghanem, O. Salines, E. Litwiller and I. Pinnau, *Polym. Chem.*, 2014, **5**, 6914–6922.
39 X. Ma, O. Salinas, E. Litwiller and I. Pinnau, *Macromolecules*, 2013, **46**, 9618–9624.
40 B. S. Ghanem, R. Swaidan, E. Litwiller and I. Pinnau, *Adv. Mater.*, 2014, **26**, 3688–3692.
41 R. Swaidan, B. Ghanem and I. Pinnau, *ACS Macro Lett.*, 2015, **4**, 947–951.
42 Y. B. Zhuang, J. G. Seong, Y. S. Do, H. J. Jo, Z. Cui, J. Lee, Y. M. Lee and M. D. Guiver, *Macromolecules*, 2014, **47**, 3254–3262.
43 Y. Hong, J. W. Lam and B. Z. Tang, *Chem. Soc. Rev.*, 2011, **40**, 5361–5388.
44 H. Tong, Y. Hong, Y. Dong, M. Haussler, J. W. Lam, Z. Li, Z. Guo, Z. Guo and B. Z. Tang, *Chem. Commun.*, 2006, 3705–3707.
45 J. E. McMurry and M. P. Fleming, *J. Am. Chem. Soc.*, 1974, **96**, 4708–4709.

 This journal is © The Royal Society of Chemistry 2016